

Large-volume single-beam dark optical trap for atoms using binary phase elements

Roei Ozeri, Lev Khaykovich, Nir Friedman, and Nir Davidson

Department of Physics of Complex Systems, Weizmann Institute of Science, Rehovot 76100, Israel

Received December 1, 1999; revised manuscript received March 21, 2000

A novel method to trap ultracold atoms in a single-beam, dark optical dipole trap, which uses a binary phase element, is proposed and demonstrated. The length and the width of this trap are independently controlled to enable a larger volume, a more symmetric shape, and a higher loading efficiency. More than 10^6 rubidium atoms were loaded into the trap at a trapping laser detuning of 0.1–10 nm above the atomic transition.

© 2000 Optical Society of America [S0740-3224(00)03406-8]

OCIS codes: 020.7010, 050.1380.

1. INTRODUCTION

Blue-detuned optical dipole traps rely on repulsive light forces to tightly confine atoms mostly in the dark, where perturbations induced by the trapping light (e.g., spontaneous scattering of photons, light-assisted losses, and distortions of the atomic energy levels) are largely reduced.^{1,2} Such dark optical traps thus enable long lifetimes at high atomic densities and long atomic-coherence times, which are important for precision spectroscopy and the study of ultracold atomic collisions and of quantum-degenerated atomic samples. The use of single-beam traps enables simple and robust dynamical changes of the trap geometry and strength (e.g., using a zoom system) that can further increase the atomic density.³ Very long atomic spin-relaxation times were recently measured in such a single-beam, blue-detuned trap based on a simple π -phase mask.²

The main disadvantage of single-beam dark optical traps is the low loading efficiency ($\sim 10^{-3}$) from the magneto-optic trap (MOT) that usually serves as the source for cold atoms. The low loading efficiency results from the very different volume and shape of the (nearly spherical) MOT and the highly elongated dipole traps. For example, for the simplest dipole trap, composed of a single Gaussian beam with waist W_0 of 10–50 μm , the characteristic length is the corresponding Rayleigh range $Z_r = \pi W_0^2/\lambda \approx 0.3\text{--}8\text{ mm}$ (for $\lambda \approx 1\text{ }\mu\text{m}$). Dark optical traps with more isotropic potentials were formed with multiple laser beams^{4,5} and demonstrated improved loading efficiency at the cost of increased complexity. Alternatively, high loading efficiencies were achieved for single-beam gravito-optical traps,^{6,7} but the reliance on the weak gravity forces prevents tight confinement for these traps. Finally, efficient loading into attractive (red-detuned) dipole traps is possible, thanks to the cooling of the atoms by the MOT beams as they fall into the dipole trap.⁸

In this paper we propose and demonstrate a novel scheme for a single-beam, dark optical dipole trap with a much larger volume and a more symmetric shape than before. We achieve this by simultaneously exploiting two

diffraction orders of a properly designed binary phase element (BPE). By improving the mode matching between the dipole potential and the MOT, we have increased the loading efficiency and hence the number of trapped atoms by a factor of 50 as compared with our previous trap² at a wide detuning range of $\delta = 0.1\text{--}10\text{ nm}$ above the $5S_{1/2}\text{--}5P_{3/2}$ transition in ^{85}Rb .

2. OPTICAL SETUP

The optical setup for the generation of our dark optical trap is illustrated in Fig. 1. An incident collimated beam impinges on a BPE and is then focused by a lens. The BPE is composed of concentric phase rings with a π -phase difference between subsequent rings, thus creating a radial grating with uniform spacing. The BPE amplitude transfer function is given by

$$U(r) = \exp\left[i \sum_{n=1}^M \pi(-1)^{n+1} \text{circ}\left(\frac{r}{a_1 + (n-1)a}\right)\right], \quad (1)$$

where M is the number of phase rings illuminated by the beam, and a is the width of all phase rings, except a_1 , which is the radius of the central phase area. In the geometrical optics limit (which is a good approximation when $M \gg 1$), the diffraction pattern of the BPE is composed of discrete diffraction orders. The 0th diffraction order is suppressed, owing to destructive interference between adjacent phase rings. Figure 1 depicts the 1st and -1 st diffraction orders from the radial grating, each having a diffraction efficiency of 40.5%,⁹ which together form an outgoing cone of light. When focused, the cone will appear in the focal plane as a narrow ring. The ring closes upon itself in both sides of the focal plane owing to the beam divergence to form a dark region completely surrounded by light. Note that the use of both the 1st and -1 st diffraction orders of the grating is essential for obtaining complete enclosure of the dark region by light.¹⁰ This is seen by comparison of the setup of Fig. 1 to a similar setup in which a refractive axicon was used to form a light cone.⁷ There, the dark region opened to one side of

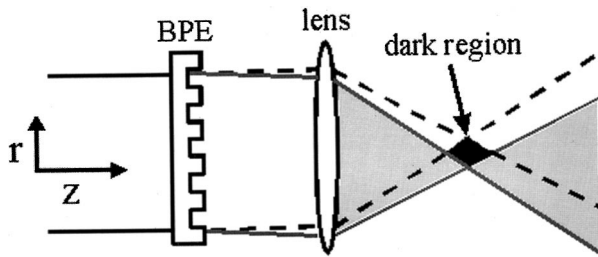


Fig. 1. Generation of a dark optical trap by use of a binary phase element (BPE). The 1st (gray) and -1st (dashed) diffraction orders are focused and form a dark volume around the focal plane, completely surrounded by light.

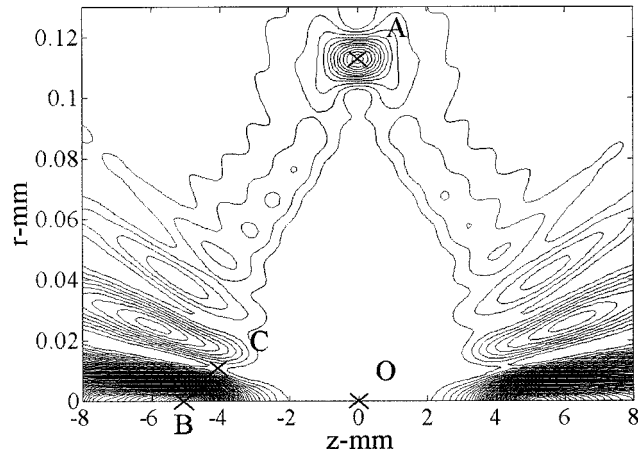


Fig. 2. Contour map for the calculated light intensity of the trap: A, transverse maximum; B, axial maximum; C, lowest barrier height; O, trap center, at the focus of the lens.

the optical axis, so additional gravitational forces were required to obtain a so-called gravito-optical trap.

For a quantitative evaluation of the light distribution around the focal region of Fig. 1, wave optics was used. Figure 2 presents a numerical solution of the Fresnel diffraction integrals for the parameters used in our experiment: a focusing lens with focal distance $f = 16$ mm, a BPE with $a = 50$ μm and $a_1 = 37.5$ μm , and an impinging Gaussian beam with wavelength $\lambda = 0.78$ μm and waist $W_{0,\text{input}} = 400$ μm . As seen, a dark volume at the focus of the lens is indeed surrounded by light in all directions. The width and the length of the dark region, $R = 0.11$ mm (OA in Fig. 2) and $Z = 5.1$ mm (OB), respectively, can be simply estimated as $R = (\pi/2)MW_{0,\text{focus}}$ and $Z = (\pi/2)MZ_r$. $W_{0,\text{focus}} = \lambda F / \pi W_{0,\text{input}}$ is the waist of the focused Gaussian beam, $Z_r = \pi W_{0,\text{focus}}^2 / \lambda$ is its Rayleigh range, and $M = W_{0,\text{input}} / a$ is the number of the radial grating periods within the incoming beam waist. The main point is that R and Z can be nearly independently controlled by use of the two parameters M and $W_{0,\text{focus}}$, as opposed to a Gaussian beam where $M = 1$, so R and Z are uniquely related.

Several new features emerge from the wave-optics picture that were missing from the ray-optics one. First, the width of the light ring at the focal plane is exactly the diffraction limit of the Gaussian beam ($W_{0,\text{focus}}$). Second, at both sides of the focal plane where the 1st and -1st diffraction orders of the BPE overlap, they interfere to form bright and dark (radial) interference fringes, which form channels with reduced dipole potential height. In par-

ticular, the dark fringe closest to the optical axis (C in Fig. 2) has a dipole potential height of only 13 μK , as opposed to the transverse potential height (A) of 154 μK of the light ring at the focal plane and to the longitudinal potential height (B) of 754 μK of the bright fringe along the optical axis (these values are calculated for a detuning of $\delta = 1.3$ nm and a trap-beam power of 120 mW). Third, the radius of the central phase region of the diffractive optical element must be carefully optimized to ensure constructive interference of the light on the focal light ring, and thus optimize the transverse potential height of the trap. The best radius was numerically found to be $a_1 = 0.75a$. Figure 3 presents the optical potential in the focal plane for $a_1 = 0.75a$ and for $a_1 = 0.25a$, which was found to give the lowest transverse potential height. As seen, an 80% improvement in the transverse potential height is achieved through this optimization.

The BPE was formed as a binary surface-relief phase element.¹¹ Glass plates were coated with photoresist (PR) by a spinner, where the spinner rotation speed was adjusted to obtain the desired thickness of the PR layer. The plates were then exposed to UV light through a mask and developed to remove the PR in the areas exposed to light all the way to the glass. Thus the thickness of the PR layer determined the phase difference between differ-

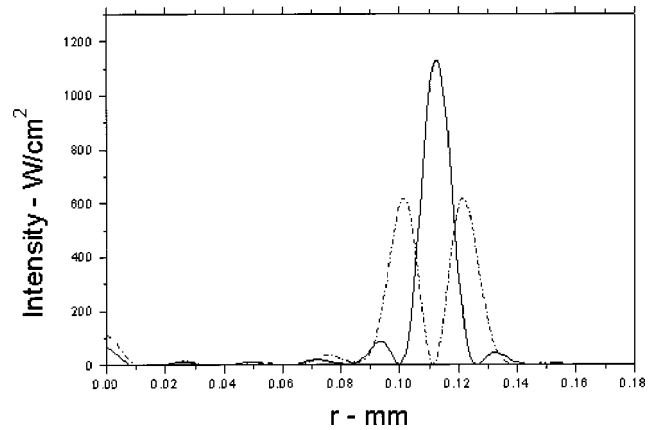


Fig. 3. Calculated trap potential at the focal plane for central phase area radius $a_1 = 0.75a$ (solid curve) and $a_1 = 0.25a$ (dashed curve).

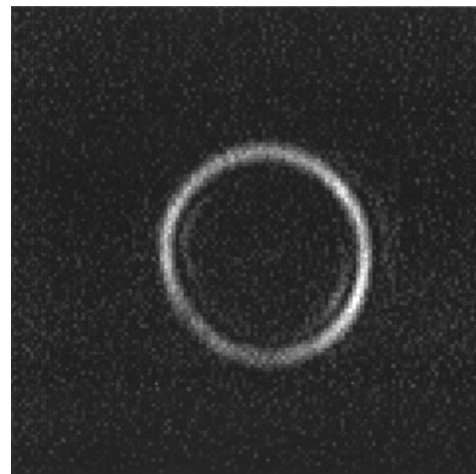


Fig. 4. CCD picture of the trap at the focal plane.

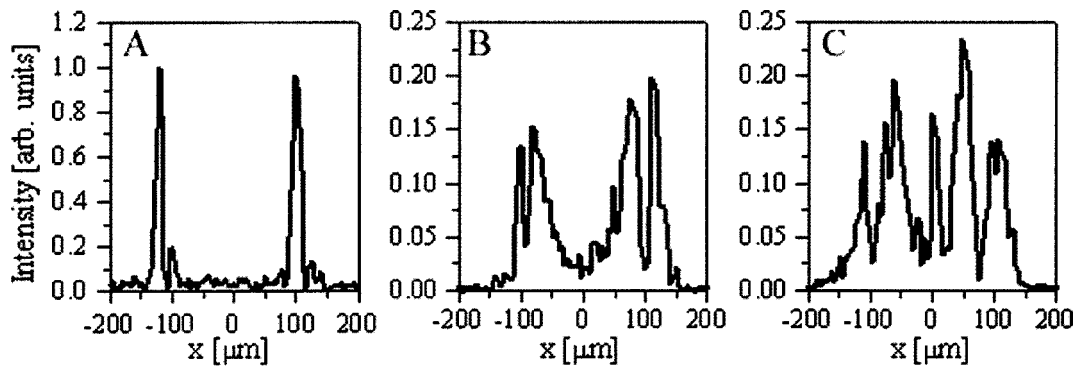


Fig. 5. Measured cross sections of the trapping light intensity, at three planes along the trap: A, focal plane ($Z = 0$); B, $Z = 1.56$ mm; and C, $Z = 2.08$ mm.

ent areas of the beam. For a π phase difference and for a PR with index of refraction $n = 1.5$, the desired thickness of the PR layer is $d = \lambda/[2(n - 1)] = 0.78 \mu\text{m}$.

A Ti:sapphire laser with a line width of ~ 40 GHz and a TEM_{00} (Gaussian) transverse mode with $W_{0,\text{input}} = 400 \mu\text{m}$ was passed through a BPE with $a = 50 \mu\text{m}$ and then focused by a lens with $f = 16$ mm. In the focal plane of the lens a $150\text{-}\mu\text{m}$ -diameter glass ball was placed to block a small 0th diffraction order of the beam (owing to inaccuracies in the PR layer thickness). The trap was then imaged into the vacuum chamber with a 1:1 magnifying telescope. A CCD camera picture of the trap at the focal plane is shown in Fig. 4. Three cross sections of the trap light intensity at different distances along the optical axis, extracted from such pictures, are shown in Figs. 5(a)–5(c) and are in a good agreement with the calculated light intensity of Fig. 2. The laser power going into the cell was 120 mW, with a total diffraction efficiency of $\sim 60\%$ of the 1st and -1 st diffraction orders of the BPE.¹² The dark focal region was aligned with the center of a MOT, which served as the cold atomic source.

3. TRAPPING OF ATOMS IN THE BINARY-PHASE-ELEMENT TRAP

The loading procedure was very similar to that described in a previous work.² Briefly, 700 ms of MOT loading, 47 ms of compression, and 3 ms of polarization gradient cooling produced a cloud of $\sim 10^8$ atoms, with a temperature of $9 \mu\text{K}$ and a peak density of $\sim 10^{11}$ atoms/cm³. After the MOT beams were shut off, a few million atoms were typically loaded into the optical trap. The number of trapped atoms was measured with fluorescence imaging into a photomultiplier tube, induced by a $100\text{-}\mu\text{s}$ laser pulse resonant with the $5S_{1/2}$, $F = 3 \rightarrow 5P_{3/2}$, $F = 4$ transition. Figure 6 shows the number of trapped atoms as a function of the trapping time for different trapping-beam detunings. As seen, for every detuning there are two different time scales for the loss of atoms from the trap: 55–80 ms and 300–350 ms. The fast decay time corresponds to atoms that are trapped only in the radial direction (two-dimensional trapping), as the lowest point in the trap potential barrier is of the order of the atomic temperature of $9 \mu\text{K}$. Hence atoms with a kinetic energy higher than the lowest point are lost after the time it will take them to traverse the trap (~ 70 ms). The slower de-

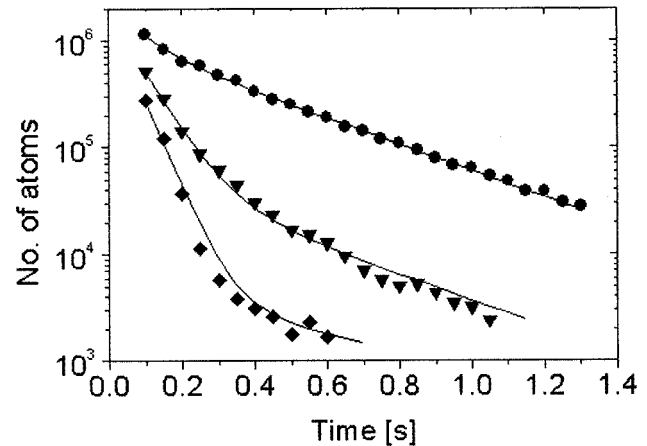


Fig. 6. Number of atoms in the trap as a function of time after the MOT turn-off, for $\delta = 1.5$ nm (circles), 3 nm (triangles), and 5 nm (diamonds). The solid curves are fits as sums of two exponentials, which give a fast decay-time constant of 55–80 ms, and a slow decay-time constant of 300–350 ms. The fraction of three-dimensional trapped atoms is 0.5, 0.03, and 0.003, for $\delta = 1.5, 3,$ and 5 nm, respectively.

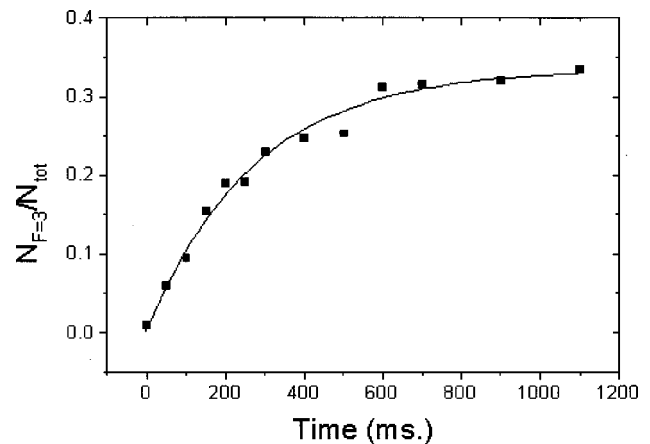


Fig. 7. Fraction of atoms in the $F = 3$ hyperfine level as a function of time, at a trapping-beam detuning of 1.3 nm. The $(1/e)$ spin-relaxation time was measured to be 273 ms.

cay time is due to atoms that are trapped in three dimensions and are lost owing to collisions with hot background atoms. The loss measurements were repeated for $\delta = 0.2\text{--}10$ nm, and the fraction of three-dimensional

trapped atoms changed from 1 for $\delta \leq 1$ nm, to $<10^{-3}$ for $\delta = 10$ nm, which supports our interpretation.

Finally, the spin-relaxation time of the atoms in the trap was determined by measurement of the rate at which the atoms undergo spontaneous Raman scattering events, which transfer the atoms between the two hyperfine levels of the ground state.² After pumping of all the atoms in the trap to the $F = 2$ hyperfine level of the ground state, the population of the $F = 3$ hyperfine level was measured as a function of time. Figure 7 shows the fraction of atoms in the $F = 3$ hyperfine level as a function of time, at a trapping-beam detuning of 1.3 nm. The $(1/e)$ spin-relaxation time was measured to be 273 ms. Using the analysis described in Ref. 2, we calculated the total photon-scattering rate to be 10 s^{-1} .

4. CONCLUSIONS

To conclude, a dark optical trap for cold atoms with improved symmetry and hence improved loading efficiency of $\sim 5\%$ was proposed, demonstrated, and characterized. The use of multiple diffraction orders from a binary phase element enabled us to construct the trap with a single laser beam and yet not to rely on gravity for confinement. This opens the possibility for us to compress the trapped atoms by dynamically changing the volume of the trap, using a fast zoom-lens system instead of the focusing lens of Fig. 1. For example, a zoom system that decreases $W_{0,\text{focus}}$ by $\times 10$ would decrease the trap volume by $\times 10^4$ and increase the potential height by $\times 100$.¹³ There could be several ways to overcome the low potential at the dark interference fringes. One could, for example, move the trap rapidly so as to form a time-averaged potential that will be the average between the destructive and constructive fringes, or alternatively, one could destroy coherence only in the azimuthal direction by using a rotating diffruser. We note that even though diffractive optical elements have certain limitations in creating three-dimensional optical potentials, they enable the formation of almost any arbitrary shape of optical potential in two dimensions. Therefore, provided that the confinement along the optical axis is achieved independently, by use of a blue-detuned standing wave, for example, interesting

two-dimensional physics that is sensitive to the potential shape, such as quantum chaos, can be studied with such elements. Finally, we estimate that nearly all the atoms from our ~ 1 -mm MOT can be loaded into a dark optical trap by use of a BPE with $M = 30$ and a 2-W-power trapping laser with a 1-nm detuning from resonance.

REFERENCES AND NOTES

1. N. Davidson, H. J. Lee, C. S. Adams, M. Kasevich, and S. Chu, "Long atomic coherence times in an optical dipole trap," *Phys. Rev. Lett.* **74**, 1311–1314 (1995).
2. R. Ozeri, L. Khaykovich, and N. Davidson, "Long spin relaxation times in a single-beam blue-detuned optical trap," *Phys. Rev. A* **59**, R1750–R1753 (1999).
3. N. Friedman, L. Khaykovich, R. Ozeri, and N. Davidson, "Compression of cold atoms to very high densities in a rotating-beam blue-detuned optical trap," *Phys. Rev. A* **61**, 031403(R) (2000).
4. T. Kuga, Y. Torii, N. Shiokawa, and T. Hirano, "Novel optical trap of atoms with a doughnut beam," *Phys. Rev. Lett.* **78**, 4713–4716 (1997).
5. Y. B. Ovchinnikov, I. Manek, and R. Grimm, "Surface trap for Cs atoms based on evanescent-wave cooling," *Phys. Rev. Lett.* **79**, 2225–2228 (1997).
6. C. G. Aminoff, A. M. Steane, P. Bouyer, P. Desbiolles, J. Dalibard, and C. Cohen-Tannoudji, "Cesium atoms bouncing in a stable gravitational cavity," *Phys. Rev. Lett.* **71**, 3083–3086 (1993).
7. Y. B. Ovchinnikov, I. Manek, A. I. Sidorov, G. Wasik, and R. Grimm, "Gravito-optical atom trap based on a conical hollow beam," *Europhys. Lett.* **43**, 510–515 (1998).
8. K. L. Corwin, S. J. M. Kuppens, D. Cho, and C. E. Wieman, "Spin-polarized atoms in a circularly polarized optical dipole trap," *Phys. Rev. Lett.* **83**, 1311–1314 (1999).
9. J. W. Goodman, *Introduction to Fourier Optics*, 2nd ed. (McGraw-Hill, New York, 1996), Chap. 7.
10. The higher diffraction orders that are not plotted in Fig. 1 carry a total of 19% of the incident beam energy but do not reach the vicinity of the dark region.
11. N. Davidson, R. Ozeri, and R. Baron, "Fabrication of binary phase surface relief optical elements by selective deposition of dielectric layers," *Rev. Sci. Instrum.* **70**, 1264–1267 (1999).
12. The reduction from the theoretical value of 81% is due to inaccuracies in the PR layer thickness and is due to Fresnel reflections from the air-to-glass and PR-to-air surfaces.
13. We recently constructed a fast zoom system with such performances, using an objective lens mounted on a piezoelectric crystal.